

# Evaluation of pathologies in concrete using optical microscopy

## Evaluación de patologías en el concreto usando microscopía óptica

Received: 21- 07 - 2016 Accepted: 06-10-2016

Carlos Andrés Bedoya Henao<sup>1</sup>  
Jorge Iván Tobón<sup>2</sup>  
Juan José Monsalve Valencia<sup>3</sup>  
Catalina Vanegas Palacio<sup>4</sup>  
Mateo Valencia Betancur<sup>5</sup>

<sup>1</sup> Geological Engineering student. National University of Colombia Headquarters Medellín.cabedoyah@unal.edu.co.

<sup>2</sup> Full Professor Director of the Cement and Construction Materials Group (CEMATCO). Department of Materials and Minerals. Faculty of Mines. National University of Colombia Headquarters Medellín.jitobon@unal.edu.co.

<sup>3</sup> Student of Mining and Metallurgy Engineering. National University of Colombia Sede Medellín.jjmonsalvev@unal.edu.co.

<sup>4</sup> Student of Mining and Metallurgy Engineering. National University of Colombia Sede Medellín.cvanegasp@unal.edu.co.

<sup>5</sup> Civil Engineering student. National University of Colombia Headquarters Medellín. mavalenciabe@unal.edu.co.

### Summary

Some traditional tests such as compression resistance, total porosity, water infiltration, among others, are useful when carrying out an analysis of pathologies in concrete that have been attacked by aggressive agents, which go against their durability. However, these classic tests lack tools to analyze how the structural and internal change of the sample was after being attacked. What evidences the need to think about other alternatives and take into account more direct tools such as microscopy, which allows a complete macro and micro analysis about the mineralogy, structure and texture, observing in detail the composition, fractures, alterations, deformations and particular signals of the samples. Thus, in this work the applicability of petrography through conventional optical microscopy is presented in the study of the degradation of concrete produced by the attack of aggressors. Results are shown such as color change in the aggregates, distortion between grain contacts, and changes in the isotropy of the cement matrix before the fire attack. Formation of secondary phases product of the replacement of ions in the matrix that generate fracture and expansion in the samples exposed to attacks by sulphate. The appearance of new phases between the matrix and the aggregates and in the fractures for the samples subjected to alkali-silica reaction. In addition, it was possible to correlate all these petrographic transformations with the losses of mechanical performance of the concrete.

**Keywords:** Pathology analysis; concrete.

### Introduction

The construction sector in Colombia, is consolidated as an important reference in the country's economy by increasing its share of GDP. This development must be accompanied by a continuous advance in science and technology of the materials used in this industry, such as

stone aggregates, bricks, cement, concrete, etc., in order to guarantee its quality and sustainability. To achieve this progress, interdisciplinary work is essential, in order to make use of the different knowledge, and in this way, make possible certain practices that suppress or give them a hand to traditional materials evaluation techniques, such as optical petrography (conventional optical microscopy) that "is a branch of the geological sciences dedicated to the scientific description and systematic classification of rocks, from an analysis in the microscope, where optical mineralogy is used which is an application of the physics of the light to the study of minerals" (Lozano, 2003; Broekmans, 2009).

Optical microscopy applied to the study of concrete is a very powerful tool when analyzing and understanding the structural behavior of this material, as well as its status, description of its components, causes of deterioration, suitability with respect to project specifications and possible future behavior. In this sense, authors such as Ingham (2009) have used optical microscopy to assess the damage caused by fire in concrete, finding that through the petrography can accurately establish the depth and intensity of damage. Some researchers (Zerbino & Glaccio, 2014; Józwiak-Niedźwiedzka, et al., 2015; Lukschová, Prikryl, & Pertold, 2009; Katayama, 2010) have used this characterization technique to evaluate the alkali-aggregate reaction in concrete, showing that the reaction can be propitiated by the presence in the mixture of reactive silica or carbonate aggregates; they have found that with this technique the cracks product of this reaction can be well defined, the material that is reacting and the product that is formed of the reaction to quantify the extent of the damage. Elsen (2006) shows how this technique is important in the concrete world to characterize the aggregates, the mineral additions, describe the pore structure, study the interfacial zone (ITZ), reaction edges between the aggregates and the cement paste, among other aspects. Sutter et al. (2006) use optical microscopy to report the formation of calcium oxychloride which is a potentially destructive phase for concrete and which is formed from the chemical interaction between magnesium chloride and hardened cement paste.

This work focused on the study of three aggressive agents that significantly deteriorate concrete and that go against its durability, such as attack by sulfates, alkali-silica reaction and fire damage. Materials and mix design are presented individually in the specimens, petrographic description in the healthy and attacked samples, results obtained and their relationship with the loss of compression resistance.

## Sulfate attack

### Materials and methods

In the elaboration of the specimens, dolomite stony aggregate was used from the area of Río Claro, Antioquia, of the company Dolomitas de Colombia S.A.S. This aggregate was crushed in order to obtain a granulometry for thick ½ "mesh trays (sizes smaller than 12.50 mm) and retained in the # 4 mesh (sizes greater than 4.75 mm), and for the thin mesh through #8 (Sizes less than 2.36 mm) and retained in the mesh # 16 (Sizes greater than 1.18 mm) according to the Colombian Technical Standard (NTC) 174.

The cement used was a type I portland cement produced by the company Cemento Argos, named within the company as a concrete material because it has a low content of mineral addition and high initial and final strength. For the manufacture of the test pieces we worked with a volume ratio of coarse aggregates, fine aggregates, cement and water of 31: 30: 11: 21 with a water cement ratio of 0.6.

A total of 9 test tubes were produced with the same mixing design, 5 of them to be subjected to attack by sulfates, of which 4 were destined for simple compression and flexure tests and one was destined for petrography, the remaining 4 for fulfill the role of healthy or control samples, 3 subjected to flexo-traction and compression tests and one to be analyzed by optical petrography.

The specimens, after demolding, were cured for 28 days according to the procedure of ASTM C 192 / C 192M - 06. After that, the selected specimens were immersed in a MgSO<sub>4</sub> solution with a concentration of 5% and a pH of 8.1 for 4 months in accordance with ASTM C1012, taking into account that this test was performed with concrete prisms but not with mortar bars as stipulated in the standard. The pH control in the samples was carried out weekly during the 4 months in order to have a controlled follow-up on the evolution of the specimens.

After 4 months, we proceeded to the analysis of the data obtained from the flexo-traction and simple compression tests in the samples attacked, followed by the manufacture of the thin sections for their petrographic analysis.

## Petrography

### Shows healthy control

Concrete sample composed of aggregates with angular to sub-angular forms of high to very low sphericity with sizes between 500  $\mu\text{m}$  and approximately 1 cm, composed of pure marble composed almost entirely of carbonate crystals with serial, bimodal and equigranular varying between 100  $\mu\text{m}$  and 5 mm. The texture in the stone aggregates is not homogeneous having polygonal grain-plastic textures with triple contacts and sutured textures. The aggregate distribution: matrix: empty is 65: 30: 5 (Figure 1). The distribution of voids is irregular, areas with more voids and irregular sizes are observed.

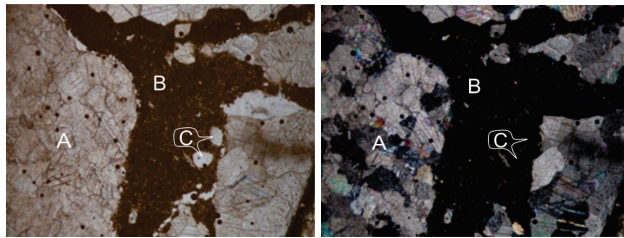


**Figure 1.** Relationship aggregates: matrix: representative voids. A-Calcareous aggregate. B-Cement paste. C-Empty. (Left nicols parallel, right crossed nicols, 4X).

The sample presents 2 types of fractures that are described below:

- **Fracture Type 1:** Irregular that cut both the aggregates and the matrix, with a maximum thickness of 350  $\mu\text{m}$ , continuous and without fillers. This type of fracture could originate during the manufacture of the thin section.
- **Fracture Type 2:** Irregular, which cut only the aggregates following partially the contacts between the grains, maximum thickness of 50  $\mu\text{m}$ , continuous and filled by the cementing matrix (Figure 2).

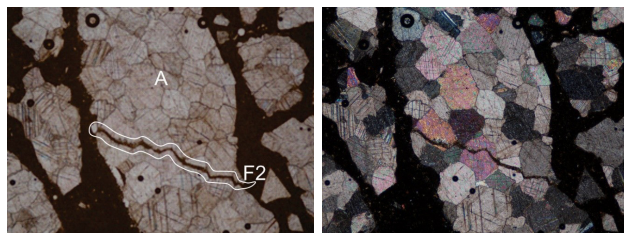


**Figure 2.** Type 2 fracture in aggregate. A- Calcium Aggregate F2- Fracture type 2 (Left parallel, nicols, nicols right crossed, 4X)

The dark brown, granular matrix, composed of low birefringence phases of approximately 15  $\mu\text{m}$  and isotropic phases. The homogeneous color in the matrix suggests a good hydration in the cement paste, and the contact with the aggregates a good adhesion between the paste and the aggregates.

### Attacked simple

Starting from the fact that the mineralogical and structural composition of the concrete is the same, only the observed changes will be emphasized.

The change in the aggregates product of the attack is incipient, although some grains are observed rotten. A secondary phase results from the ionic replacement in the cementitious matrix, colorless, of low relief, with very low birefringence, of irregular edges, disseminated, and forming straight planar structures sub parallel through the matrix. Associated with this was the growth of a second phase, colorless, of medium relief and medium birefringence (Figure 3).

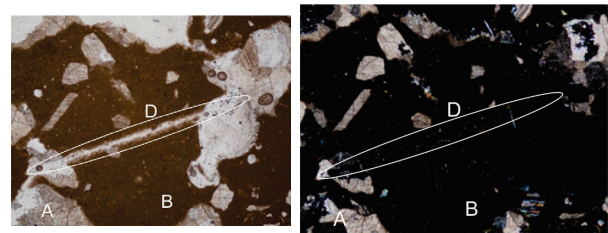


**Figure 3.** Secondary phases formed and slight increase in anisotropic phases in the matrix. A- Calcareous aggregate. B- Cement paste. D- Secondary Phase replacing the matrix. (Left parallel nicols, right crossed nicols, 10X).

Fractures in the matrix are observed in the samples, forming bridges between the aggregate grains, slightly sinuous, with a maximum thickness of 20  $\mu\text{m}$ , of little extension, and some filled by the secondary phase described above. This type of fracture can be associated with the secondary phase formed, with some of the fractures perpendicular to the planar structures (Figure 4).

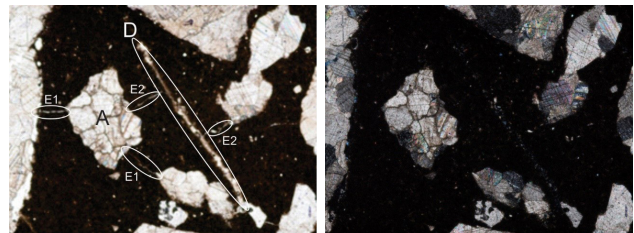


**Figure 4.** Association between phases and fractures A- Calcareous aggregate. D- Secondary phase. E1- Fractures between grains. E2. Fractures associated with the formation of the phase. (Left parallel nicols, right crossed nicols, 10X).

## Analysis and discussion

The secondary phases observed by optical microscopy make reference to the formation of gypsum, bruce and silica gel, as has been described by authors such as Collepari (2003) magnesium sulphate decalcifies the CSH from the cement paste to form the In the phases found, during this process the concrete presents an important loss of mechanical strength.

Gypsum formation also contributes to the loss of strength of the cement matrix, as well as contributing to the volumetric expansion of the paste.

Cement under the attack of sulphate (Santhanam, Cohen, & Olek, 2003), so the microcracks perpendicular to the planar structures are associated with the formation of this mineralogical phase.

The damage registered in the concrete is not relevant in the observation time, the homogeneity of the cement paste is conserved, the adhesion between aggregates and matrix is consistent, the fissures do not have a considerable thickness and length, and the mineralogical evolution characteristic of the attack is not advanced.

## Alkali-Silica Reaction

### Materials and methods

In the elaboration of the specimens, a quartz sandite and chert, an aggregate from the El Roble mine, located in the department of Chocó, Colombia, was used as a reactive siliceous aggregate. It was decided to work with this material due to its use in previous studies, for being of siliceous and microcrystalline or cryptocrystalline composition, factor that increases the susceptibility to react with the cement paste. The aggregates were crushed with the objective of obtaining a granulometry for thick thickened mesh  $\frac{1}{2}$  "(less than 12.50 mm) and retained in the # 4 mesh (greater than 4.75 mm), for the fines mesh was used # 8 (less than 2.36 mm) and retained in the # 16 mesh (greater than 1.18 mm) according to NTC 174. We worked with only these two sizes in the aggregates because the material used is not for commercial use, therefore, the granulometric curve specified in the standards was not available; This factor, added to the fact that the objective of this project is not to design a mixture, with specific granulometry, was then chosen for these two grain sizes. The cement used is

a portland type I cement with an alkaline content of 0.45. For the manufacture of the test pieces we worked with a volume ratio of coarse aggregates, fine aggregates, cement and water of 31: 33: 11: 21 with a water cement ratio of 0.6.

A total of 9 specimens with the same mix design were manufactured, 5 of them to be subjected to the reaction, of which 4 were destined to simple flexo traction and compression tests and one was destined to petrography, the remaining 4 to comply with the role of healthy control samples, 3 subjected to flexo traction and compression tests and one to be used for petrography.

The procedure for submitting the samples to the reaction was based on ASTM C1293-08b where although it is used to evaluate the expansion in mortar bars due to the alkali-silica reaction, it has a correlation with the reactions between the cement alkalis and the siliceous components of the aggregates, so it served as a support to attack the samples of concrete used in this study. To accelerate the reaction, NaOH was added to the mixing water, which according to ASTM C1293-08b is equivalent to 1.25% of the mass of the cement. The specimens after demolding were cured for 28 days according to the procedure of ASTM C 192 / C 192M-06 and the specimens destined to be attacked were stored controlling the temperature and humidity of the environment, according to the norm, for 4 months.

After 4 months, we proceeded to analyze the data obtained from the flexo traction and simple compression tests in the samples attacked, followed by the manufacture of the thin sections for their petrographic analysis.

## Petrography

### Shows healthy control

Concrete sample composed of aggregates of sandite quartz and some chert grains with angular to sub angular forms of medium to very low sphericity with sizes between 500  $\mu$ m to 1 cm approximately, almost entirely made up of quartz crystals and in a lesser proportion feldspar, Muscovite and matrix partially recrystallized to biotite with inequigranular size distribution. The texture in the stone aggregates is homogeneous having clastic textures with point to planar contacts. The aggregate distribution: matrix: empty is 75: 20: 5 (Figure 5). The distribution of voids is irregular, areas with more voids and irregular sizes are observed.

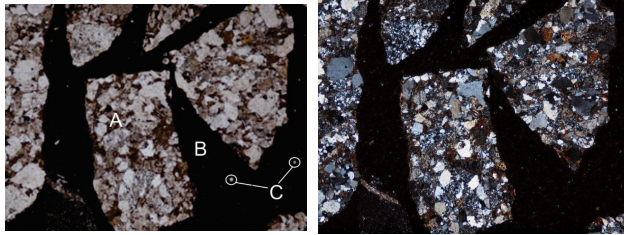


**Figure 5.** Relationship aggregates: matrix: representative voids. A- Siliceous Aggregate. B- Cement paste. C- Empty. (Left nicols parallel, right crossed nicols, 4X).

The sample shows a type of fracture that affects only the matrix. Irregular, moderately sinuous, of average thickness 5 mm and without filling (Figure 6).

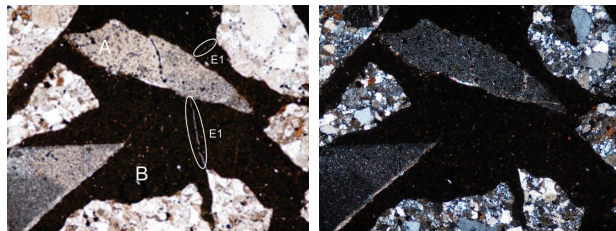


**Figure 6.** Micro fractures in the cementing matrix. A- Siliceous Aggregate. B- Cement paste. E1- Micro fractures between aggregate grains. (Left nicols parallel, right crossed nicols, 4X).

The matrix is grayish-brown, granular, composed mostly of isotropic phases and, to a lesser extent, by phases of low and medium birefringence of approximately 15 mm. Again the homogeneous color in the matrix suggests a good hydration in the cement paste, and the contact with the aggregates a good adhesion between the paste and the aggregates (Figure 5).

### Attacked simple

The most significant change is marked by the appearance of a colorless, low relief, low birefringence phase, formed between the cementitious matrix and the aggregate, cutting this in some cases (Figure 7). This corresponds to the formation of alkaline silicates, which are the main result of this reaction, which has the characteristic of being expansive and soluble in water, so its formation is detrimental to the mechanical properties and durability of concrete.

The fractures observed are of the same type as those described above in the healthy section.

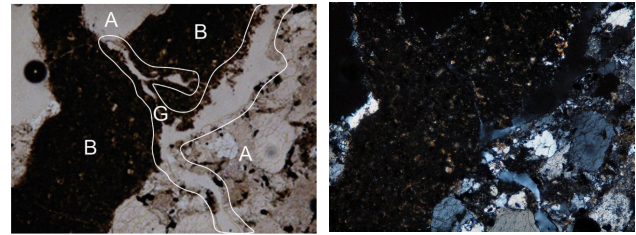


**Figure 7.** Formation of limiting secondary phase between the aggregate and the matrix. A- Siliceous Aggregate. B- Cement paste. G- Secondary phase formed in the matrix-aggregate limit (Left parallel nicols, right crossed nicols, 10X).

## Analysis and discussion

Manifestations of calcium silicate gels were observed in only 1% of the sample, the cement paste retained its homogeneity, the adhesion between aggregates and cement paste is good, and without relevant fracturing, which indicates the little effect of the reaction in this concrete under the conditions evaluated.

### Attack by fire

## Materials and methods

In the elaboration of the specimens, dolomite stony aggregate from Rio Claro, Antioquia, from the company *Dolomitas de Colombia S.A.S.* Thanks to the bibliographic review that was developed, it was concluded that this aggregate would be the best option to perform the attack because the calcareous aggregates when heated show a change in coloration and generally become CaO, thus affecting the mechanical properties of concrete (Guise, 1997). The design of the mixture used in the manufacture of the specimens was the same as in the sulphate attack.

9 test tubes were manufactured, 5 of them to be attacked and 4 of control. Three of the control samples after having been properly cured were each subjected to a flexo traction test and two single compression tests according to ASTM C293 and ASTM C109 in order to obtain supporting data.

After the 5 samples ready to be attacked were properly cured for 28 days according to the procedure of ASTM C 192 / C 192M - 06, the attack was carried out, this was done in a direct flame oven in order to simulate a fire The samples were taken at 400 ° C and kept at this temperature for 10 min. Here the samples F400-1 and F400-2 are taken. 12 min later the oven reaches 800° C and there the self-regulating

procedure is repeated for 10 min and finally samples F800-1 and F800-2 are taken out.

After the burning, we proceeded to the analysis of the data obtained from the flexo traction and simple compression tests in the attacked samples, followed by the manufacture of the thin sections and duly the petrographic analysis of them.

## Petrography

### Shows healthy control

Since the specimens manufactured for this attack have the same characteristics as those used in the attack by sulfate, it refers to the analysis of the healthy control section.

### Sample attacked at 400 °C

Concrete sample defined by isotropic aggregates with heterogeneous forms that vary from sub-rounded to predominantly slender angles, varying in size from 650 mm to 17.46 mm. The aggregate proportion: matrix: empty is 60:30:10. The lithology corresponding to the aggregates is homogeneous, composed of dolomite characterized by having a bimodal distribution in the grain sizes with means of 160 and 400 mm with an irregular granular texture defined by contacts between the concave-convex, sutured and locally polygonal grains with points. Triples (Figure 8). Occasionally, trace minerals are identified as low birefringence and high relief, accompanying the dolomite among the aggregates; On the other hand, in the spaces between the aggregates and the matrix, a mineral with a vetiform shape, with a siliceous appearance of low birefringence and low relief, is identified.

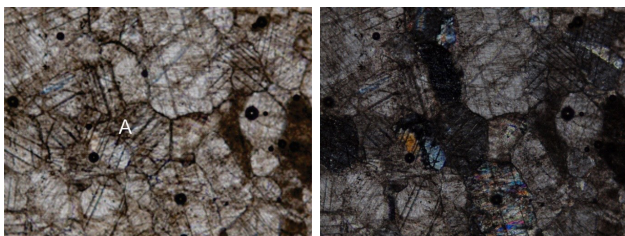


**Figure 8.** Contact between grains in the Dolomite. Zone not affected. A- Calcareous aggregate (left parallel nicoles, crossed right nicoles, 4X).

The matrix is described as a paste of very fine particles of yellowish brown coloring towards the edges in contact with the voids and more brown in the center of the matrix. The relationship between the aggregates and the matrix is defined by discrete contacts taking a darker coloration in the matrix.

The fracture that presents the sample is in the matrix without affecting the aggregates and is characterized by being generally unfilled, sinuous, and vary its thickness between 10 and 30 mm.

Punctually in the area attacked the matrix shows a change in coloration where it becomes darker and a slight distortion in the contact of the grains is observed (Figure 9).

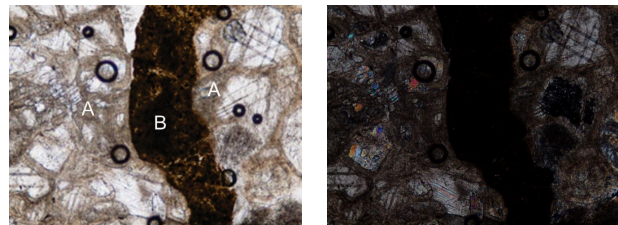


**Figure 9.** Attack zone A- Calcareous aggregates with distorted grain contacts. B- Cement paste of heterogeneous color, slightly uniform and darkened. (Left parallel nicoles, right crossed nicoles, 10X).

### Sample attacked at 800 °C

Concrete sample defined by isotropic aggregates with heterogeneous forms that vary from sub-rounded to predominantly slender angles, varying in size from 450 mm to 13.75 mm. The aggregate ratio: matrix: empty is 60:25:15. The lithology corresponding to the aggregates is homogeneous composed by dolomite characterized by presenting a bimodal distribution in grain sizes with averages of 150 and 450 μm with an irregular granular texture defined by contacts between concave-convex grains, sutured, locally polygonal with points triples and more punctually scattered contacts not very defined (Figure 10).

The matrix is described as a paste of very fine particles, of dark brown coloration, with more dark brown specks towards the center of the matrix. The relationship between the aggregates and the matrix is defined by discrete contacts taking a darker coloration in the matrix. The fracture presented by the sample is in the matrix without affecting the aggregates and is characterized by being generally unfilled, sinuous, and varying its thickness between 15 and 40 mm (Figure 10).

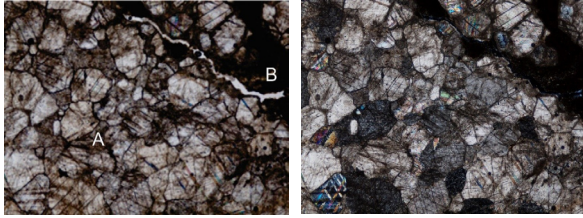


**Figure 10.** Contact between grains in the Dolomite. Zone not affected. A- Calcareous aggregate. B- Cement Paste (Left parallel, nicoles crossed, nicoles crossed, 4X).

In the attacked zone, the aggregates have a much more dark brown coloration, with apparent loss of the property of extinction, distortion in the contact of grains and burns in some of these; the matrix shows porous spaces, zones of wear and areas of very dark blackish coloration (Figure 11).

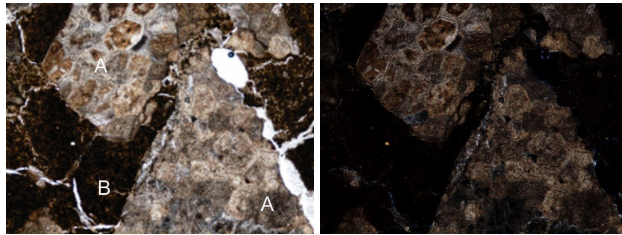


**Figure 11.** Attack zone Dark, porous and cracked matrix; Contact of distorted grains and burnt grains. A- Calcareous aggregate burned. B- Cement Paste (left parallel, nicoles crossed, nicoles crossed, 10X).

## Analysis and discussion

The petrographic examination showed an increase in the fracturing of the cement paste, intensifying it towards the periphery of the sample, due to a slow detachment that occurs in the form of fractures parallel to the surface affected by the fire, leading to a gradual separation of the concrete layers (Ingham, 2009). There is a loss in the adherence between the aggregates and the cement paste, with fracturing and separation between them, given that the grain-matrix limits act as planes of weakness against attack.

Despite having noticed a distortion between the contacts of grains and a quasi-calcination of the aggregates as the temperature increased, compared to what was seen (Koca et al., 2006), at 800 ° C the texture is still slightly preserved and structure of the rock, however, the mineralogy of the aggregate is almost unrecognizable at this temperature. The distortion between grain contacts can generate a significant loss in the aggregate resistance due to a decrease in the contact area, losing structure and load capacity, which may suggest a relationship between the grain size of the aggregate and the loss of resistance in concrete attacked by fire.

The color in the aggregates varied from a pale orange in the specimens of 400 ° C to a red brown in the 800 ° C samples, relating the increase in temperature with the development of the reddish color in the aggregates (Ingham, 2009; Purkiss & Guise, 2001).

At 400 ° C (Figure 9), the matrix presents an uneven color and with anisotropic phases, however, at 800 ° C a complete isotropy and a uniform black color are observed (Figure 11), this happens because after at 500 ° C the cement matrix becomes completely anisotropic (Ingham, 2009).

## Mechanical behavior

Table 1 shows the values of resistance to flexion and compression, exhibited both by the altered samples and in the undisturbed ones (not subjected to attack). This for the 3 attacks described above.

**Table 1.** Summary of average resistance measures in MPa

		Sulfates	Alkali silice	Fire
Flexión	Unaltered	7.82	7.51	7.63
	Attacked	7.73	6.79	3.62
Compression	Unaltered	36.72	33.72	35.11
	Attacked	33.86	28.23	10.24

The results indicate that the greatest change in terms of mechanical properties was presented in the samples exposed to fire attack. Its resistance to compression has a loss of 70.8% with respect to the original value, a fact that would be fatal for any civil structure.

In second place of deterioration is the concrete subjected to the alkali-silica reaction where with only 1% alkaline silicates formation in the total mass of the sample, there is a loss of compressive strength of 16.3%.

The attack by sulphates evaluated affected the mechanical properties of the concrete, especially the resistance to compression, reducing it by 7.8%.

In all the samples the visual damage is highlighted, wear and discolorations are observed, characteristics that indicate a superficial damage in the concrete. By bringing this into the context of a civil work, it could be reflected in a deterioration of the concrete's coating, and with this, a greater failure against external agents.

## Conclusions

In the petrography it was possible to see that the biggest change was presented by the samples exposed to the fire with the increase of fracturing and planes that favor the failure of the concrete, with changes in the composition and in the optical properties of the cement paste and with the distortion of the contacts between the grains. This was very well reflected in its mechanical properties, where practically its resistance was reduced to one third only by being subjected to 800 ° C which is a normal temperature in most fires, this fact would be fatal for any civil structure and It could be seen in the petrography.

The formation of gypsum, brucite and silica gel was evidenced as secondary phases as a result of the reaction of C-S-H with sulphate ions, as well as their association in the expansion of concrete. However, in the short term, the damage in the concrete product of the sulphate attack was found to be the least aggressive of the three analyzed, probably due to the low concentration of the aggressor agent in the medium and the short duration of the test. Even with the low amount of secondary phases formed in the attack by sulfates, the compression resistance had a loss of 7.8% with respect to the concrete that was not subjected to the attack.

The alkali-silica reaction produced around the chert grains the formation of alkaline silicates, this phase at the time of evaluation came to be only 1% of the volume of paste, however, in terms of resistance to compression meant a fall in 16.3% with respect to the control sample.

Through petrographic techniques, it is possible to demonstrate, differentiate and characterize the pathologies present in concrete samples that have been attacked with agents that go against their durability. Similarly, changes and behaviors between healthy concrete and concrete affected by these attacks can be determined. In addition, it is possible to establish correlations between the petrographic alterations and the mechanical performance of these materials.

## References

ASTM International, (2013) ASTM C192 / C192M - 13a Standard Practice for Making and Curing Concrete Test Specimens in the Laboratory.

ASTM International, (2013) ASTM C109 / C109M -13e1 "Standard Test Method for

Compressive Strength of Hydraulic Cement Mortars (Using 2-in. or [50-mm] Cube Specimens).

ASTM International, (2010) ASTM C293 / C293M-10 "Standard Test Method for Flexural Strength of Concrete (Using Simple Beam With Center-Point Loading).

ASTM International, (2002) ASTM C1012 - 02 Standard Test Method for Length Change of Hydraulic Cement Mortars Exposed to a Sulfate Solution.

ASTM International, (2008) ASTM C1293 - 08b Standard Test Method for Determination of Length Change of Concrete Due to Alkali Silica Reaction.

Broekmans, M. A. (2009). Petrography as an essential complementary method in forensic assessment of concrete deterioration: Two case studies. *Materials Characterization*, 644-654.

Collepardi, M. (2003). A state-of- the-art review on delayed ettringite attack on concrete. *Cement and Concrete Composites*, 401-407.

Elsen, J. (2006). Microscopy of historic mortars— a review. *Cement and Concrete Research*, 1416-1424.

Guisse, S. E. (1997). The use of color image analysis for assessment of fire damaged concrete. *PhD thesis Aston University*. Birmingham: Department: Civil Engineering and Mechanical Engineering.

Ingham, J. (2009). Application of petrographic examination techniques to the assessment of fire-damaged concrete and masonry structures. *Materials Characterization*, 700-709.

Jóźwiak-Niedźwiedzka, D., Gibas, K., Brandt, A. M., Glinicki, M. A., Dąbrowski, M., & Denis, P. (2015). Mineral composition of heavy aggregates for nuclear shielding concrete in relation to alkali-silica reaction. *Procedia Engineering*, 162-169.

- Katayama, T. (2010). The so-called alkali-carbonate reaction (ACR) — Its mineralogical and geochemical details, with special reference to ASR. *Cement and Concrete Research*, 643–675.
- Koca, M., Ozden, G., Yavuz, A., Kincal, C., Onargan, T., & Kucuk, K. (2006). Changes in the engineering properties of marble in fire-exposed columns. *International Journal of Rock Mechanics and Mining Sciences*, 520–530.
- Lozano, J. E. (2003). Petrography, a tool for quality control and diagnosis. Retrieved from *Revista Universidad Nacional de Colombia*: <http://revistas.unal.edu.co/index.php/email/article/view/1182>
- Lukschová, Š., Príkryl, R., & Pertold, Z. (2009). Petrographic identification of alkali–silica reactive aggregates in concrete from 20th century bridges. *Construction and Building Materials*, 734–741.
- Santhanam, M., Cohen, M., & Olek, J. (2003). Effects of gypsum formation on the performance of cement mortars during external sulfate attack. *Cement and Research*, 325–332.
- Short, N., Purkiss, J., & Guise, S. (2001). Assessment of fire damaged concrete using colour image analysis. *Construction and Building Materials*, 9–15.
- Sutter, L., Peterson, K., Touton, S., Van Dam, T., & Johnston, D. (2006). Petrographic evidence of calcium oxychloride formation in mortars exposed to magnesium chloride solution. *Cement and Concrete Research*, 1533–1541.
- Zerbino, R., & Glaccio, S. (2014). Evaluation of alkali–silica reaction in concretes with natural rice husk ash using optical microscopy. *Construction and Building Materials*, 132–140.